

## A Nested Square Shaped Metasurface-Based Broadband Linear Polarization Converter for Ku-Band Applications

Yunus KAYA<sup>1\*</sup>

<sup>1</sup>Bayburt University, Department of Electricity and Energy, Bayburt 69000, Turkey  
(ORCID: [0000-0002-2380-5915](https://orcid.org/0000-0002-2380-5915))



**Keywords:** Ku-band, Metasurface, Broadband, Linear polarization converter.

### Abstract

This paper presents a wideband, thin, low-cost, and easy to fabricate linear polarization (LP) converter design utilizing metasurface (MS) for Ku-band (12-18 GHz) applications (also in the 18-19 GHz part of the K-band (18-27 GHz)). The design has a topology on a 1.6 mm thick FR-4 dielectric material with copper MS on the front and an entirely copper slab on the back. The presented design shows a polarization conversion ratio (PCR) of beyond 90% within the 12-19 GHz frequency band and also over 99% in the 12.5-13.1 and 16.32-17.64 GHz frequency ranges. To further give insight into the physical structure of the suggested MS-based polarization converter (PC), both the  $u-v$  axes are analyzed, and the existing surface behaviors at resonance frequencies are investigated. We compare the performance outputs with other Ku-band PCs, and the efficiencies of the suggested strategy over current MS-based LP converters are emphasized.

### 1. Introduction

The polarization condition for an electromagnetic (EM) wave expresses the aspect of the swing of the electric field part at a constant point in the free space, taking time into account. The polarization converter (PC) has the competency to alter the EM wave direction. Manipulation of the polarization status of the EM wave has received great attention because of its popular application areas, such as communication and remote perception [1]. PCs among the polarization manipulation equipment have proven the importance of EM wave PC from the microwave frequency region to the THz frequency region with several applications such as radar cross field degradation in invisibility technology [2], [3] and antenna design [4], [5]. Traditionally, polarization conversion is achieved by the effect of birefringence in crystals found in nature [6]. The weak anisotropies, bulkiness, large power losses, and angle-dependent polarization responses of these crystals limit their practical use. In order to eliminate these disadvantages, metasurface (MS) structures have recently been used in diverse applications. Examples of such applications are excellent lenses [7], an

invisibility cloak [8], a superior absorber [9], and a PC [10]. So far, PCs relying on MS structures have been utilized in the microwave [10], infrared [11], and visible regimes [12], [13] due to their flexible and easy profile.

In general, PCs may be developed to perform in transmission [14] and/or reflection status [15]. PCs with the transmission mode necessitate multi-layer mechanisms, making their fabrication a very difficult task and a time-consuming component [16]. Meanwhile, PCs with reflective mode may be seen in a single-layer with metallic material-dielectric substrate material-metallic material setting [17]. Particularly, the manageable design style of reflective mode PCs [13], [17]-[22] on a single-layer moving in a linear manner has obtained significant interest. Another attractive property of a reflective PC design is the extension of the bandwidth to be appropriate in practice.

In this study, a single-layer, thin, low-cost, and MS-based broadband reflective linear polarization (LP) converter is designed specifically for Ku-band studies. The suggested converter includes an MS structure designed on the front side of a dielectric substrate material (FR-4) and a ground

\*Corresponding author: [ykaya@bayburt.edu.tr](mailto:ykaya@bayburt.edu.tr)

Received: 19.12.2022, Accepted: 03.03.2023

plane with metallic termination on the back surface. The efficiency of the suggested idea was tested through a set of simulations in comparison to Ku-band PCs using crescent-shaped MS [19], double crescent-shaped MS [20], fishbone-shaped MS [21], and two-corner-cut square patch MS [22]. The suggested converter ensures an LP conversion with a polarization conversion ratio (PCR) bigger than 90% all over the Ku-band (microwave band of frequencies from 12 to 18 GHz), as well as in the 18-19 GHz part of the K-band (microwave band of frequencies from 18 to 27 GHz). Therefore, this design can be simply implemented for Ku-band microwave applications.

## 2. Material and Method

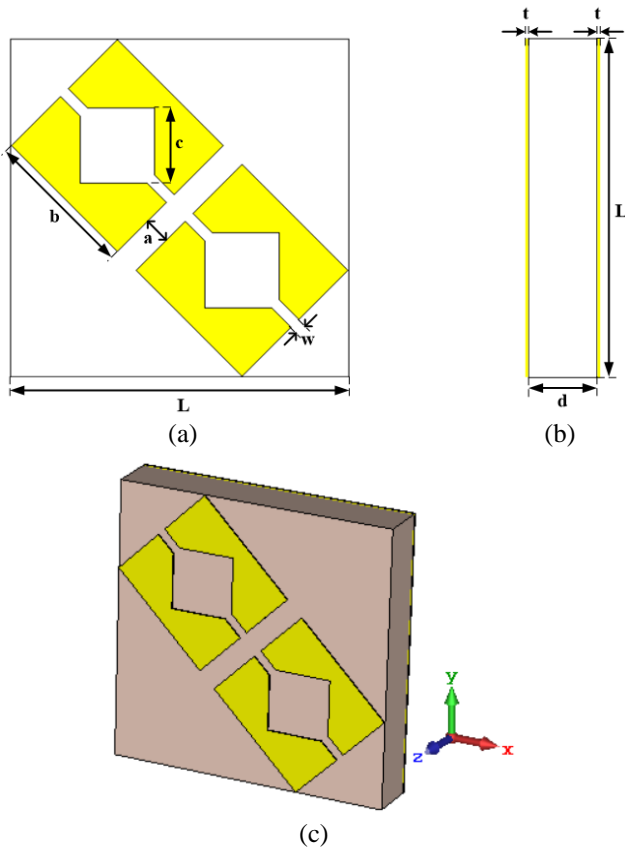


**Figure 1.** The suggested LP converter with (a) front view, (b) left side view, and (c) coordinate system layout with three-dimensional representation.

The suggested LP converter is designed on a substrate material with an MS on the front side and an all-metal termination on the back surface. Copper (with its electrical conductivity  $\sigma = 5.8 \times 10^7$  S/m) was selected for MS and metal finishing, respectively, located on the front and back surfaces of the substrate. The substrate in the middle part is FR-4 dielectric material (the relative dielectric constant ( $\epsilon_r$ ) is 4.3 and the loss tangent ( $\tan\delta$ ) is 0.025), which is easily available on

the market. The thickness of the copper is  $t = 0.035$  mm and the thickness of FR-4 material is  $d = 1.6$  mm. The shape of the MS consists of two symmetrical nested squares (additionally, the nested square shape consists of one filled and the other empty square), with the distance between the two symmetrical shapes  $a = 0.7$  mm, and the other dimensions in Figure 1 are  $L = 9$  mm,  $b = 4$  mm,  $c = 2$  mm, and  $w = 0.3$  mm.

To clarify the basis of the process of the suggested PC, it is necessary to conduct some EM analysis. It is assumed that the EM wave propagates to the MS-based PC in the +z-direction with the y-polarized electric field intensity ( $E_y$ ) and the harmonic dependence  $e^{j\omega t}$  in time ( $\omega$ : angular frequency), the incident wave ( $E_i$ ) in the phasor space is defined as follows.

$$\vec{E}_i = a_y E_y e^{-jkz} \quad (1)$$

Here  $k$  is the wave number. For LP conversion, the EM wave with an electric field component in the y-direction will be reflected in the same direction (y-direction – co-polarization) or in the direction normal to the incident plane (x-direction – cross-polarization) after hitting the MS. In this scenario, the reflected wave ( $E_r$ ) is given as follows.

$$\vec{E}_r = (a_x E_{rx} + a_y E_{ry}) e^{jkz} \quad (2)$$

Here,  $E_{rx}$  and  $E_{ry}$  are the components of the electric field intensity of the reflected wave in the x- and y-directions, respectively. Likewise,  $E_{ix}$  and  $E_{iy}$  are the components of the electric field intensity of the incident wave in the x- and y-directions, respectively; the co-reflection coefficient –  $R_{yy}$  and the cross-reflection coefficient –  $R_{xy}$  for the wave polarized in the electric field intensity y-direction are denoted as follows.

$$R_{yy} = \frac{E_{ry}}{E_{iy}} \text{ and } R_{xy} = \frac{E_{rx}}{E_{iy}} \quad (3)$$

With the usage of  $R_{yy}$  and  $R_{xy}$  coefficients in Equation (3), the PCR value of the LP for the y-polarized incident wave may be obtained as follows [18]-[22].

$$\text{PCR} = \frac{|R_{xy}|^2}{|R_{xy}|^2 + |R_{yy}|^2} \quad (4)$$

Here  $|*|$  denotes the magnitude of “\*”. In addition, to deeply understand the physical operation of the LP concept for the suggested design, the y-polarized incident wave was separated in the u – v axes, which is shown in Figure 2.

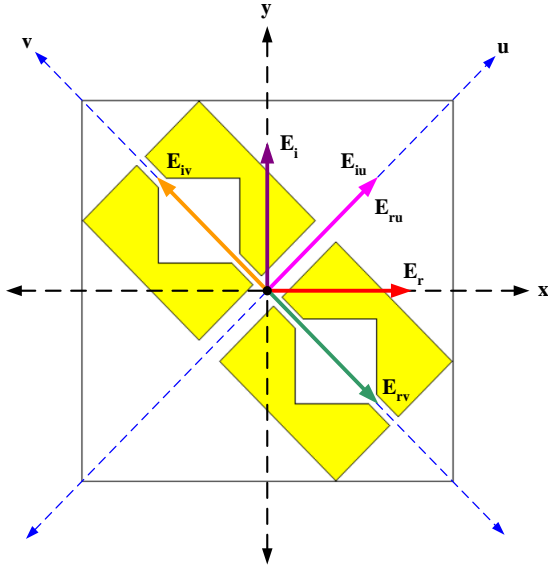


**Figure 2.** Decomposition of incident ( $E_i$ ) and reflected wave ( $E_r$ ) into u- ( $E_{iu}$  and  $E_{ru}$ ) and v-axes ( $E_{iv}$  and  $E_{rv}$ ) for the suggested design.

In Figure 2,  $E_{iu}$  and  $E_{iv}$  represent the electric field intensity parts of the incident wave in the u- and v-directions, respectively, and similarly,  $E_{ru}$  and  $E_{rv}$  represent the electric field intensity components in the u- and v-directions of the reflected wave, respectively. Accordingly, the incident and reflected wave ( $E_i$  and  $E_r$ , respectively) may be stated by decomposing into the u- and v-axes [18], [20]:

$$\vec{E}_i = a_u E_{iu} e^{j\phi_{iu}} + a_v E_{iv} e^{j\phi_{iv}} \quad (5)$$

$$\vec{E}_r = a_u r_{uu} E_{iu} e^{j\phi_{ru}} + a_v r_{vv} E_{iv} e^{j\phi_{rv}} \quad (6)$$

In Equations (5) and (6),  $\phi_{iu}$  and  $\phi_{iv}$  denote the phases of the incident wave in the u- and v-directions, respectively, and similarly,  $\phi_{ru}$  and  $\phi_{rv}$ , the phases of the reflected wave in the u- and v-directions, respectively. Additionally, here  $r_{uu}$  and  $r_{vv}$  are reflection coefficients in the u- and v-directions, respectively, and are expressed as follows.

$$r_{uu} = \frac{E_{ru}}{E_{iu}} \text{ and } r_{vv} = \frac{E_{rv}}{E_{iv}} \quad (7)$$

For the LP conversion, according to Figure 2, the components in the +u- and +v-directions must be reflected in the +u- and –v-directions with the same amplitude. So,  $|r_{uu}|$  and  $|r_{vv}|$  must be equal to 1. In addition,  $\phi_{uu} = 0^\circ$  must be since the incident wave in the +u-direction is reflected in the +u-direction. Similarly,  $\phi_{vv}$  must be equal to  $-180^\circ$  in order for the incident wave in the +v-direction to be reflected in the –v-direction. Therefore, the reflection coefficients in the u- and v-directions for the x-polarized reflection of the y-polarized wave, that is, for the LP conversion,  $|r_{uu}| \cong |r_{vv}| \cong 1$  and phase difference  $\Delta\phi = |\phi_{uu} - \phi_{vv}| = 180^\circ$  must be.

### 3. Results and Discussion

#### 3.1. Simulation Results

The suggested MS-based LP converter, whose geometry is given in Figure 1, was created in the CST Microwave Studio program as shown in Figure 1(c). The simulations were conducted in the frequency domain, in the 7-21 GHz frequency range, and by choosing the tetrahedral mesh type. Accordingly, the co- and cross-reflection coefficients for the suggested PC design are presented in Figures 3(a) and 3(b) in terms of dB and amplitude, respectively. As seen in Figure 3(a), MS resonates at 12.776 and 17.016 GHz, and the  $R_{xy}$  is around  $-1.1$  dB while the  $R_{yy}$  is below  $-11$  dB in the 12-19 GHz frequency band. From Figure 3(b), it is noted that the  $|R_{yy}|$  and  $|R_{xy}|$  given as amplitudes are below 0.28 and above 0.87, respectively, within the specified frequency range. Figure 3(d) shows the PCR data obtained using Equation (4). As seen in Figure 3(d), PCR is over 90% in the 12-19 GHz frequency band. Additionally, the PCR value is over 99% in the frequency ranges of 12.5-13.1 and 16.32-17.64 GHz.

The reflection coefficients ( $|r_{uu}|$  and  $|r_{vv}|$ ) and phases ( $\phi_{uu}$ ,  $\phi_{vv}$ , and  $\Delta\phi$ ) in the u – v directions of the suggested design are given in Figures 4(a) and 4(b), respectively. It can be noted from Figure 4(a) that LP is achieved (12-19 GHz frequency range) and at other frequencies, the  $|r_{uu}|$  and  $|r_{vv}|$  in the u – v axes are roughly equal to 1. In addition, from Figure 4(b), which shows the phase differences in the u- and v-directions, it is noted that the phase difference in the u – v directions is roughly  $180^\circ$  ( $\Delta\phi = |\phi_{uu} - \phi_{vv}| = 180^\circ$ ) in the frequency range of 12-19 GHz.

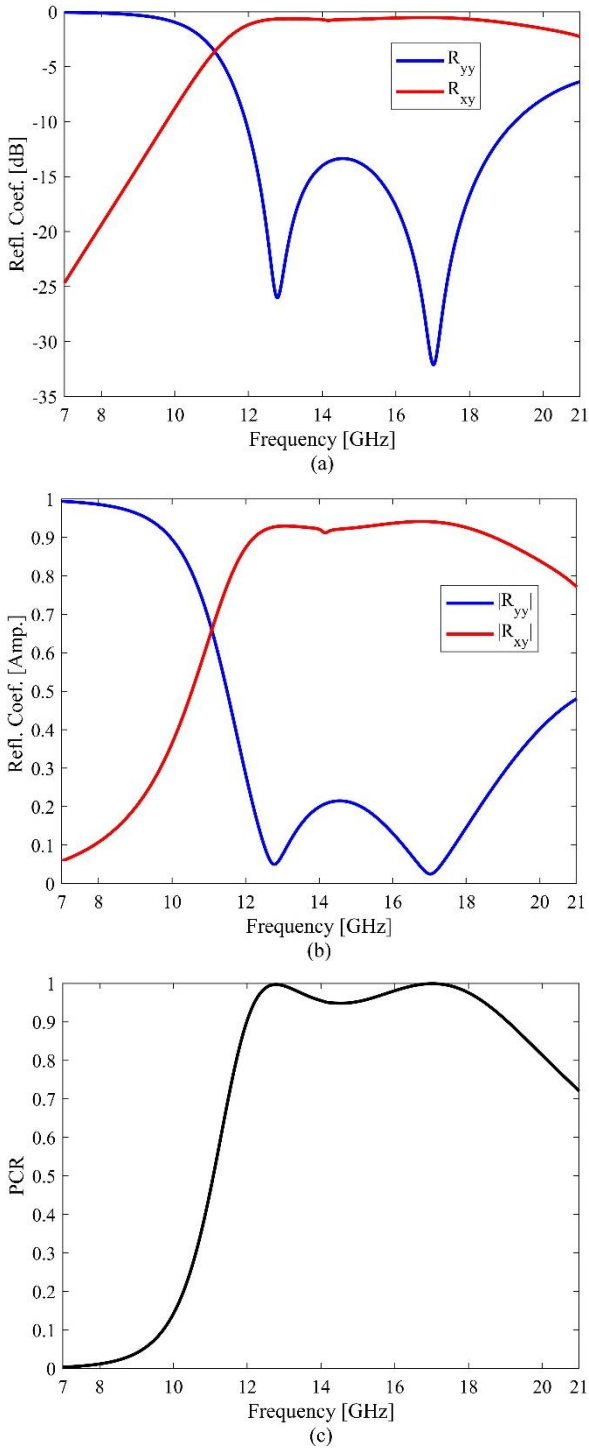


**Figure 3.** In the 7-21 GHz frequency range of the suggested PC; (a) reflection coefficient in dB ( $R_{yy}$  and  $R_{xy}$ ), (b) reflection coefficient in amplitude ( $|R_{yy}|$  and  $|R_{xy}|$ ), and (c) PCR value.

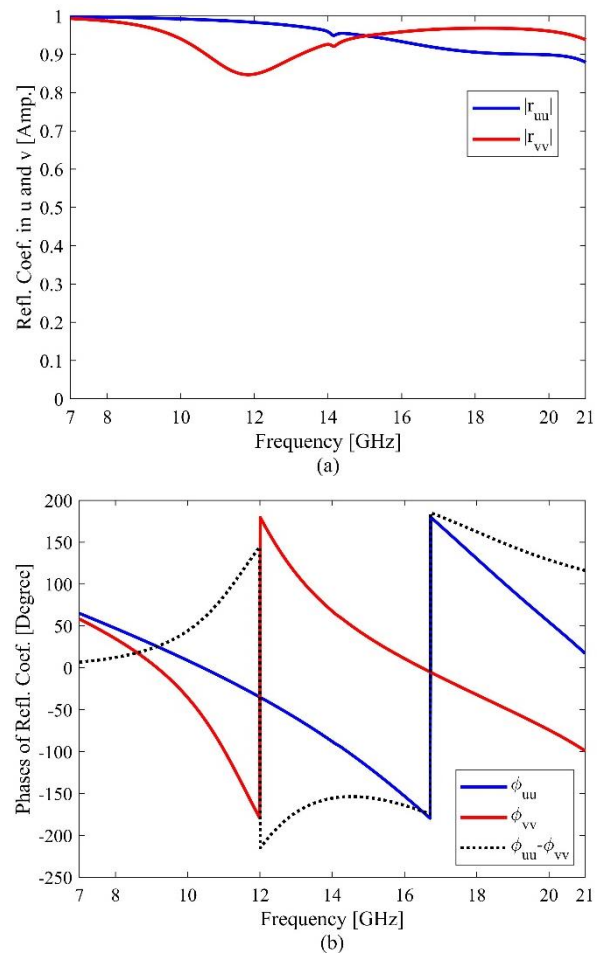


**Figure 4.** (a) Reflection coefficients ( $|r_{uu}|$  and  $|r_{vv}|$ ) and (b) phases ( $\phi_{uu}$ ,  $\phi_{vv}$ , and  $\Delta\phi$ ) in the u – v directions of the suggested PC.

When the EM wave is sent to the MS-based PC, electrical and magnetic polarizations occur on the structure. This polarization causes the generation of electric and magnetic currents. In this context, surface current behaviors on metal parts (MS and metal termination) were investigated at resonance frequencies to know the physical mechanism of the suggested PC and to further examine its performance and effectiveness. Accordingly, Figures 5(a)- 5(d) show the surface currents in MS and metal termination at resonance frequencies, namely 12.776 and 17.016 GHz. When Figure 5(a) and Figure 5(c) are examined together, it is seen that the surface currents at 12.776 GHz are anti-parallel, and when Figures 5(b) and 5(d) are examined together, the surface currents at 17.016 GHz are also anti-parallel. This shows that the suggested MS-based LP converter design has a magnetic resonance at both resonance frequencies, namely 12.776 GHz and 17.016 GHz (on the contrary, the parallelism of the currents would indicate electrical resonance at the mentioned frequency).



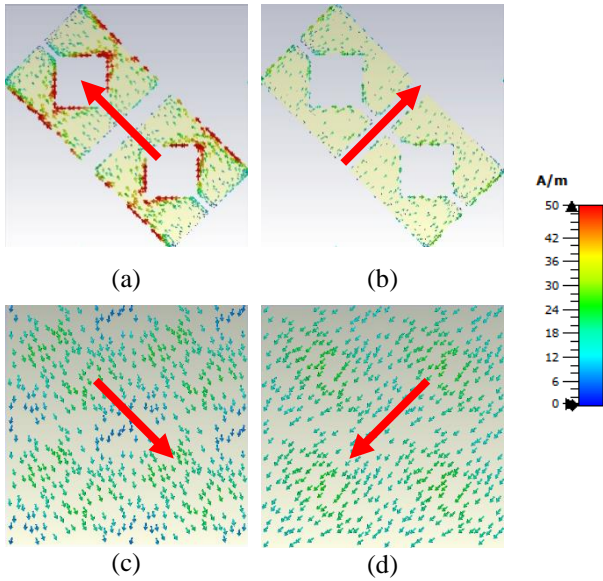


**Figure 5.** Distributions of surface currents for (a), (b) MS and (c), (d) metal termination for resonance frequencies of 12.776 and 17.016 GHz, respectively.

### 3.2. Discussion

The suggested PC's conversion performance was compared with other reference Ku-band LP converters [19]-[22] in terms of conversion bandwidth, substrate type, and substrate thickness, as

shown in Table 1. The suggested design provides LP conversion with a wider bandgap than [19] and [20] in terms of conversion bandwidth. In fact, the suggested design provides LP conversion in the entire Ku-band (a microwave band of frequencies from 12 to 18 GHz) as well as in the 18-19 GHz part of the K-band (a microwave band of frequencies from 18 to 27 GHz). When the studies made according to the thickness in terms of wavelength are examined, the suggested design is 36% less thick than [22]. In terms of substrate thickness, the suggested design is thinner than both [21] and [22]. Therefore, the suggested design can be used for applications requiring thinner material. In addition, FR-4 dielectric was used as the substrate material in the suggested design, and it is both cheaper and more available than the F4-B substrate material used in [20] and [22]. This reduces the manufacturing complexity of our design. Therefore, the suggested design can be produced effectively at a lower cost than [20] and [22]. Looking at the PCR efficiency, all reference LP converters in Table 1 have a PCR value of 90%. In addition, while the MS-based LP converter we recommend has more than a 90% PCR value in the 12-19 GHz frequency range, it has a PCR value of over 99% in the 12.5-13.1 and 16.32-17.64 GHz frequency ranges.

**Table 1.** Comparison of the suggested PC with reference Ku-band LP converters [19]-[22]

Study	Conversion Bandwidth [GHz]	Substrate Thickness	Substrate Type	PCR Efficiency
[19]	12-18	1.6 mm (0.064 $\lambda$ )	FR-4	90%
[20]	11.9-18.05	1.5 mm (0.059 $\lambda$ )	F4-B	90%
[21]	9.24-17.64	2 mm (0.061 $\lambda$ )	FR-4	90%
[22]	10-18.4	3 mm (0.100 $\lambda$ )	F4-B	90%
Suggested Design	12-19	1.6 mm (0.064 $\lambda$ )	FR-4	90%

### 4. Conclusion

In this study, an LP converter operating in the 12-19 GHz frequency range for microwave Ku-band applications was suggested and validated by using the CST Microwave Studio program. The suggested PC provides over 90% PCR in the 12-19 GHz frequency range, as well as over 99% in the 12.5-13.1 and 16.32-17.64 GHz frequency ranges. In the suggested design, an easily accessible 1.6 mm thick FR-4 dielectric

material is used as the substrate. For this reason, the suggested design can also be used in cases where very thin applications are required, with a thickness of 0.064 $\lambda$ . The suggested design is a single structure. This reduces the production's complexity.

### Statement of Research and Publication Ethics

The study is complied with research and publication ethics.

### References

- [1] N. K. Grady, J. E. Heyes, D. R. Chowdhury, Y. Zeng, M. T. Reiten, A. K. Azad, A. J. Taylor, D. A. R. Dalvit, and H. T. Chen, "Terahertz metamaterials for linear polarization conversion and anomalous refraction," *Science*, vol. 340, no. 6138, pp. 1304-1307, Jun. 2013.

- [2] Y. T. Jia, Y. Liu, Y. J. Guo, K. Li, and S. X. Gong, "Broadband polarization rotation reflective surfaces and their applications to RCS reduction," *IEEE Transactions on Antennas and Propagation*, vol. 64, no. 1, pp. 179-188, Jan. 2016.
- [3] P. Su, Y. J. Zhao, S. L. Jia, W. W. Shi, and H. L. Wang, "An ultra-wideband and polarization-independent metasurface for RCS reduction," *Scientific Reports*, vol. 6, art. no. 20387, Feb. 2016.
- [4] C. F. Yang, X. W. Zhu, P. F. Liu, W. Hong, H. L. Feng, and Y. H. Shi, "A circularly polarized horn antenna based on an FSS polarization converter," *IEEE Antennas and Wireless Propagation Letters*, vol. 19, no. 2, pp. 277-281, Feb. 2020.
- [5] Q. Zheng, C. J. Guo, G. A. E. Vandenbosch, and J. Ding, "Low-profile circularly polarized array with gain enhancement and RCS reduction using polarization conversion EBG structures," *IEEE Transactions on Antennas and Propagation*, vol. 68, no. 3, pp. 2440-2445, Mar. 2020.
- [6] A. J. Danner, T. Tyc, and U. Leonhardt, "Controlling birefringence in dielectrics," *Nature Photonics*, vol. 5, no. 6, pp. 357-359, Jun. 2011.
- [7] J. B. Pendry, "Negative refraction makes a perfect lens," *Physical Review Letters*, vol. 85, no. 18, pp. 3966-3969, Oct. 2000.
- [8] D. C. Liang, J. Q. Gu, J. G. Han, Y. M. Yang, S. Zhang, and W. L. Zhang, "Robust large dimension terahertz cloaking," *Advanced Materials*, vol. 24, no. 7, pp. 916-921, Feb. 2012.
- [9] N. I. Landy, S. Sajuyigbe, J. J. Mock, D. R. Smith, and W. J. Padilla, "Perfect metamaterial absorber," *Physical Review Letters*, vol. 100, no. 20, art. no. 207402, May 2008.
- [10] H. L. Zhu, S. W. Cheung, K. L. Chung, and T. I. Yuk, "Linear-to-circular polarization conversion using metasurface," *IEEE Transactions on Antennas and Propagation*, vol. 61, no. 9, pp. 4615-4623, Sep. 2013.
- [11] Z. J. Zhang, J. Luo, M. W. Song, and H. L. Yu, "Large-area, broadband and high-efficiency near-infrared linear polarization manipulating metasurface fabricated by orthogonal interference lithography," *Applied Physics Letters*, vol. 107, no. 24, art. no. 241904, Dec. 2015.
- [12] Q. T. Li, F. L. Dong, B. Wang, F. Y. Gan, J. J. Chen, Z. W. Song, L. X. Xu, W. G. Chu, Y. F. Xiao, Q. H. Gong, and Y. Li, "Polarization-independent and high-efficiency dielectric metasurfaces for visible light," *Optics Express*, vol. 24, no. 15, pp. 16309-16319, Jul. 2016.
- [13] Z. H. Fang, H. Chen, D. An, C. R. Luo, and X. P. Zhao, "Manipulation of visible-light polarization with dendritic cell-cluster metasurfaces," *Scientific Reports*, vol. 8, art. no. 9696, Jun. 2018.
- [14] F. Costa and M. Borgese, "Systematic design of transmission-type polarization converters comprising multilayered anisotropic metasurfaces," *Physical Review Applied*, vol. 14, no. 3, art. no. 034049, Sep. 2020.
- [15] B. M. Zhang, C. H. Zhu, R. Zhang, X. F. Yang, Y. Wang, and X.M. Liu, "Dual-band wide-angle reflective circular polarization converter with orthogonal polarization modes," *Sensors*, vol. 22, no. 24, art. no. 9728, Dec. 2022.
- [16] S. M. A. M. H. Abadi and N. Behdad, "Wideband linear-to-circular polarization converters based on miniaturized-element frequency selective surfaces," *IEEE Transactions on Antennas and Propagation*, vol. 64, no. 2, pp. 525-534, Feb. 2016.
- [17] X. F. Yang, T. Qi, Y. H. Zeng, X. M. Liu, G. Lu, and Q. Cai, "Broadband reflective polarization rotator built on single substrate," *Electronics*, vol. 10, no. 8, art. no. 916, Apr. 2021.
- [18] X. Gao, X. Han, W. P. Cao, H. O. Li, H. F. Ma, and T. J. Cui, "Ultra-wideband and high-efficiency linear polarization converter based on double V-shaped metasurface," *IEEE Transactions on Antennas and Propagation*, vol. 63, no. 8, pp. 3522-3530, Aug. 2015.
- [19] T. Q. H. Nguyen, T. K. T. Nguyen, T. Q. M. Nguyen, T. N. Cao, H. L. Phan, N. M. Luong, D. T. Le, X. K. Bui, C. L. Truong, and D. L. Vu, "Simple design of a wideband and wide-angle reflective linear polarization converter based on crescent-shaped metamaterial for Ku-band applications," *Optics Communications*, vol. 486, art. no. 126773, May 2021.
- [20] X. K. Yang, Z. Ding, and Z. P. Zhang, "Broadband linear polarization conversion across complete Ku band based on ultrathin metasurface," *AEU International Journal of Electronics and Communications*, vol. 138, art. no. 153884, Aug. 2021.
- [21] Q. Zheng, C. J. Guo, H. X. Li, and J. Ding, "Broadband radar cross-section reduction using polarization conversion metasurface," *International Journal of Microwave and Wireless Technologies*, vol. 10, no. 2, pp. 197-206, Mar. 2018.

- [22] B. Q. Lin, X. Y. Da, J. L. Wu, W. Li, Y. W. Fang, and Z. H. Zhu, "Ultra-wideband and high-efficiency cross polarization converter based on anisotropic metasurface," *Microwave and Optical Technology Letters*, vol. 58, no. 10, pp. 2402-2405, Oct. 2016.